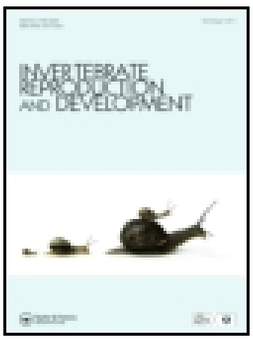

Invertebrate Reproduction & Development

ISSN: 0792-4259 (Print) 2157-0272 (Online) Journal homepage: https://www.tandfonline.com/loi/tinv20

Fine structure of the subitaneous eggshell of the sessile rotifer *Stephanoceros millsii* (Monogononta) with observations on vesicle trafficking in the integument during ontogeny

Rick Hochberg, Hui Yang, Elizabeth J. Walsh & Robert L. Wallace

To cite this article: Rick Hochberg, Hui Yang, Elizabeth J. Walsh & Robert L. Wallace (2019): Fine structure of the subitaneous eggshell of the sessile rotifer *Stephanoceros millsii* (Monogononta) with observations on vesicle trafficking in the integument during ontogeny, Invertebrate Reproduction & Development

To link to this article: https://doi.org/10.1080/07924259.2019.1581097

Published online: 22 Feb 2019.

INVERTEBRATE REPRODUCTION & DEVELOPMENT
https://doi.org/10.1080/07924259.2019.1581097

Fine structure of the subitaneous eggshell of the sessile rotifer *Stephanoceros millsii* (Monogononta) with observations on vesicle trafficking in the integument during ontogeny

Rick Hochberg [a], Hui Yang [a], Elizabeth J. Walsh [b] and Robert L. Wallace [c]

[a]Department of Biological Sciences, University of Massachusetts Lowell, Lowell, MA, USA; [b]Department of Biological Sciences, University of Texas, El Paso, TX, USA; [c]Department of Biology, Ripon College, Ripon, WI, USA

ABSTRACT

Rotifers that engage in cyclical parthenogenesis produce two types of eggs: subitaneous eggs that hatch as clonal females and meiotic eggs that hatch as haploid males, or if fertilized, as females after a period of diapause (resting eggs). The ultrastructure of resting eggshells is known for some motile species, but there are limited data on subitaneous eggshells, and no data on any eggshells of sessile rotifers. Here, we investigated the ultrastructure of the subitaneous eggshell of the sessile rotifer *Stephanoceros millsii* and its potential origins of secretion, the maternal vitellarium and embryonic integument. We also explored secretory activity in the larval and adult integuments to determine whether activity changes during ontogeny. The eggshell consists of a single layer with two sublayers: an external granular sublayer apparently derived from the maternal vitellarium, and an internal flocculent sublayer secreted by the embryonic integument that may form a hatching membrane or glycocalyx. Secretory activity remains high in both the larva and adult and appears to be the source of the thickening glycocalyx. Altogether, the subitaneous eggshell of *S. millsii* is the thinnest among monogonont rotifers. Thin eggshells may have evolved in response to the added protection provided by the mother's extracorporeal tube.

ARTICLE HISTORY
Received 11 December 2018
Accepted 3 February 2019

KEYWORDS
Asexual; cyclic parthenogenesis; embryogenesis; freshwater; indirect development; larva

Introduction

Reproduction in rotifers has been a source of investigation for over a century (Wallace et al. 2006, 2015), in large part because some taxa (Bdelloidea) appear to have evolved in the absence of sexual reproduction (e.g. Mark Welch et al. 2009), while others (Monogononta) engage in the complex process of cyclical parthenogenesis (Birky and Gilbert 1971). The latter phenomenon is complicated because of the diversity of environmental cues that trigger or modulate physiological changes in asexual (diploid) females to produce diploid eggs that hatch as sexual females. These females produce meiotic eggs that, if unfertilized, become haploid males, but if fertilized, develop into diploid female zygotes that undergo developmental arrest (Gilbert 1974; Ricci 2001; Boschetti et al. 2005, 2011). These diapausing embryos, often termed resting eggs (RE), are resistant to environmental assaults such as freezing and drying (Snell 1987; Gilbert 2003, 2004). REs have received a great deal of attention due to their importance in dispersal (Lopes et al. 2016; Rivas et al. 2018), adding genetic variability to existing populations (Gómez and Carvahlo 2001), and rebuilding populations from egg banks in sediments; e.g. on a seasonal basis or after temporary ponds evaporate and then refill (Hairston 1996; Walsh et al. 2014; reviewed in, 2017).

To date, knowledge of oogenesis in rotifers is largely focused on the external factors and endogenous signals that regulate cyclical parthenogenesis and mixis (e.g. Birky and Gilbert 1971; Gilbert 2002; reviewed by Snell 2011; Stelzer 2017). While details of oogenesis are known for a few species that have been studied by multiple researchers for over a century (e.g. Jennings 1896; Tannreuther 1920; Nachtwey 1925; Hsu 1956a, 1956b; Lechner 1966; Bentfield 1971a; Amsellem and Ricci 1982; Gilbert 1983; Pagani et al. 1993; Boschetti et al. 2005; Smith et al. 2010), data on eggshell secretion are relatively rare. The underlying processes that contribute to eggshell secretion and ultrastructure are poorly known (reviewed by Gilbert 1983) and to date have only been investigated in a few species of Bdelloidea (Amsellem and Ricci 1982; Clément and Wurdak 1991) and Monogononta (Bentfield 1971a, 1971b; Wurkdak et al. 1978; Clement 1980; Clément and Wurdak 1991; Gilbert 1995; Munuswamy et al. 1996). The germovitellarium (germarium plus vitellarium) is a syncytial organ surrounded by a follicular layer of undetermined function. Eggshell precursors flow from the vitellarium to the germarium through syncytial

CONTACT Rick Hochberg rick_hochberg@uml.edu Department of Biological Sciences, University of Massachusetts Lowell, Lowell, MA, USA

connections and lead to the eventual deposition of shell layers around the oocyte only after it separates from the germarium (Clément and Wurdak 1991). Membrane-bound vesicles traffic eggshell products (cortical granules) to the surface of the oocyte and begin depositing the shell (Bentfield 1971a, 1971b), but it is not known how long this process continues during embryogenesis. In the case of REs, which have received the most attention, the shell is multilayered and includes an internal chitinous envelope and two additional layers, the outermost of which forms various ornaments such as knobs and spines (Gilbert 1983; Clément and Wurdak 1991). By comparison, information on the secretion and structure of subitaneous (asexual) eggshells, which are fast hatching and important for quickly increasing population size, is limited. The shells of these eggs are generally thinner and less elaborate compared to resting eggs, though some species can have a complex ultrastructure (e.g. *Synchaeta pectinata* Ehrenberg, 1832) (Gilbert 1995); other species, such as *Asplanchnopus multiceps* (Schrank, 1793), can have an ornate morphology that includes a highly filamentous covering (Wurdak 2017).

To date, there is no information on the ultrastructure of any sessile rotifer's subitaneous eggshells or the maternal vitellarium that presumably secretes the eggshell precursors. Unlike other rotifers whose eggs hatch as juveniles, sessile species have indirect development that involves a larval stage (Wallace et al. 2006, 2015). Thus, the subitaneous eggs of sessile species are usually oviposited into the adult's extracorporeal tube (Figure 1(a,b)), hatch into non-feeding, female larvae that leave the parent (Figure 1(c,d)), swim for a time, settle on a submerged plant (Young et al. 2019), and begin the dual processes of secreting a new extracorporeal tube while metamorphosing to the adult stage (Kutikova 1995; Hochberg and Hochberg 2015). While the amictic eggs of sessile rotifers hatch quickly, like those of other rotifers, we posit that their eggshells might have a different ultrastructure than the asexual eggshells of motile species because the former are protected by the mother's extracorporeal tube and may not require extra shell layers or a thick shell. The eggs of motile species are either oviposited on select surfaces (Gilbert 1981; Walsh 1989) or are carried (Wallace et al. 2015); in both cases, these eggs would appear to be more exposed to environmental stresses and predation and may therefore require a more complex and layered eggshell morphology. Based on these ideas, we hypothesized that species with extracorporeal tubes may produce subitaneous eggs with very simple (e.g., thin) eggshells compared to motile species.

We further hypothesize that eggshell secretion is not limited to the maternal vitellarium in sessile rotifers. Resting eggs are known to secrete eggshell granules that are synthesized by the Golgi apparatus, but their relative contribution to the entire eggshell is not well known (Gilbert 1983). In the case of rapidly developing amictic rotifers, we predict that some eggshell precursors are also produced by the embryo, but this secretion likely comes from the integument that forms very early during development (Gilbert 1989; Hochberg pers. obs.). We further suspect that the levels of integumental secretion may differ during the ontogeny of sessile rotifers (i.e., embryo, larva, adult). All rotifers are known to have an active, secretory integument based on numerous ultrastructural observations that show abundant membrane-bound vesicles and high levels of exocytosis (Storch and Welsch 1960; Brodie 1970; Koehler 1965; Schramm 1978; Hochberg et al. 2015, 2017). In each life stage of a sessile rotifer, we predict that this vesicle trafficking will change to meet the demands of their specific environments: shell production in the embryonic environment, glycocalyx production in the larval environment (plankton), and tube production in the sessile, adult environment (periphyton). Thus, the second aim for this study was to determine whether there are qualitative and/or quantitative differences in the trafficking of membrane-bound (secretory) vesicles from embryogenesis through adulthood. To do this we used transmission electron microscopy (TEM) to explore the ultrastructure of the integument in a single late-stage asexual embryo (~1 hr prior to hatching), two larvae (free-swimming and newly settled), and a reproductive adult (few days old) (Figure 1).

Materials and methods

Stephanoceros millsii (Kellicott, 1885) was collected from submerged plants at Flint Pond, Tyngsboro, Massachusetts USA (42° 40'29.00" N, 71° 25'32.21" W) in July 2017 and 2018. Photographs of live specimens were taken on a Zeiss A1 compound microscope equipped with differential interference contrast (DIC) and a Sony Handycam digital camera. Adults were cultured in native pond water for a few days to produce asexual larvae. A single adult carrying an asexual egg, and two larvae from the same adult, were anaesthetized with 0.5% bupivacaine for 30 mins and fixed in 2.5% glutaraldehyde in 0.1 M cacodylate buffer (pH 7.3) for 2 hrs. These specimens were next rinsed in buffer (4 × 15 min) and postfixed in 1% OsO_4 in 0.1 M cacodylate buffer for 1 hr, followed by a rinsed in 0.1 M buffer (4 × 15 min), and then dehydrated in an ethanol series (70, 90, 100, 100%) for 10 min each. Specimens were embedded in Spurr's low viscosity resin. Resin blocks were sectioned on a Reichart ultramicrotome at 70 nm and silver sections were collected on copper grids. Grids were stained with uranyl acetate (3 min)

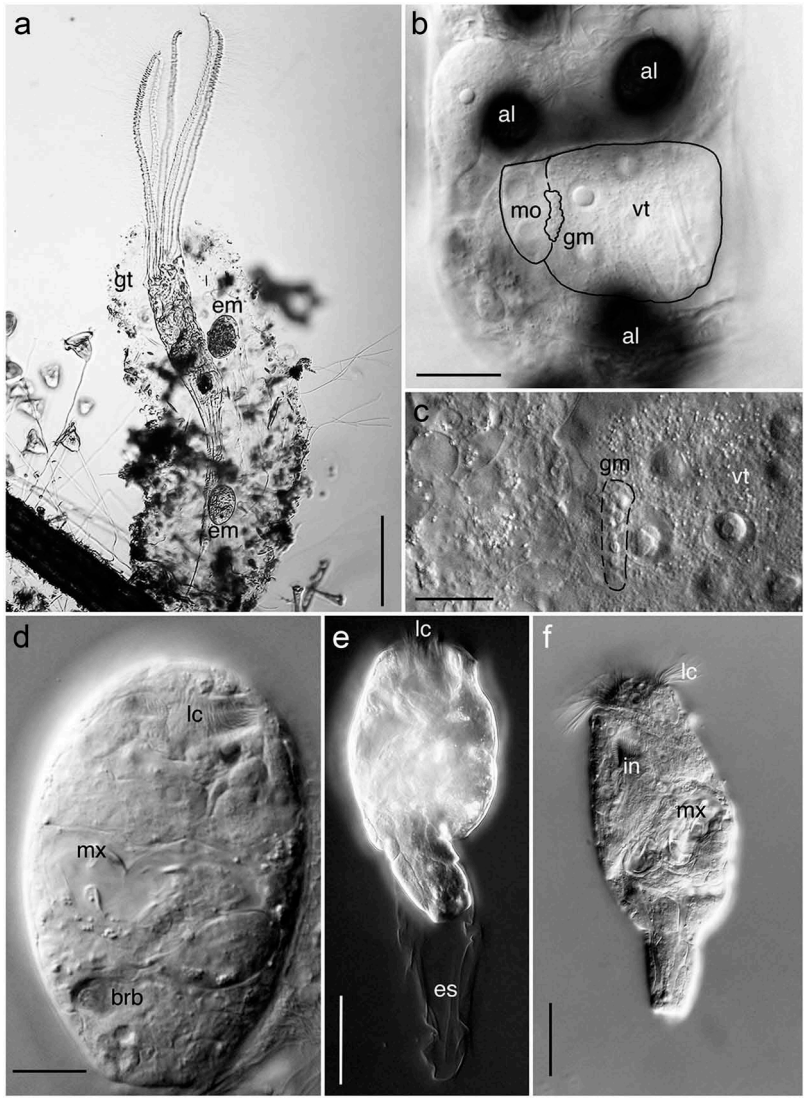

Figure 1. Life stages of *Stephanoceros millsii*. (a) Adult female in its hydrogel tube containing subitaneous (amictic) eggs. (b) DIC image of the female reproductive system (artificially outlined) showing the vitellarium (not completely in focus), germarium with tiny oocytes, and two maturing oocytes. (c) Close up of germarium (artificially outlined) from B showing the linear arrangement of tiny oocytes at the edge of the vitellarium. (d) Shelled embryo at the approximate same stage of development as the specimen examined with TEM. (e) Asexual female larva escaping the eggshell. (f) Female larva, approximately 3–4 hours posthatch.

Abbreviations: al: unicellular algae (not in focus); brb: birefringent bodies; em: asexual embryo; es: eggshell; gm: germarium; gt: hydrogel tube; in: infundibulum; lc: larval corona; mo: maturing oocytes; mx: mastax; vt: vitellarium. Scale bars = A: 200 µm; B: 30 µm; C: 15 µm; D: 20 µn; E: 40 µm; F: 60 µm.

and lead citrate (3 min) and examined on a Philips CM10 TEM and photographed with a Gatan Orius 813 digital camera (Gatan Inc., Pleasonton, CA, USA) at the University of Massachusetts Medical School in Worcester, Massachusetts. Multiple sections were examined for one adult, two eggs, and two larvae.

Digital images were cropped and minimally enhanced for brightness and contrast. ImageJ© was used to make measurements of various organelles and used to measure the length of the integument in TEM micrographs. The length of the integument was used as the basis for quantifying the number of membrane-bound vesicles per unit area. When measurements were made, n-values indicate the number of sections that were examined across all comparable specimens; e.g., eggs or larvae.

Results

Maternal vitellarium

The vitellarium is a large organ that can be located by the presence of extremely large nuclei (ca. 10 µm diameter) when visualized with DIC microscopy (Figure 1(b)). The vitellarium of a single adult, asexual female had a slightly rectangular shape containing 16–18 nuclei. On its medial margin was the germarium, which consisted of ~30 very

small (1 µm) oocytes that formed a stacked, linear cluster (Figure 1(b,c). At least two oocytes were in the process of maturing on its periphery (Figure 1(b)). At the ultrastructural level, the vitellarium was found to be syncytial and the nuclei were the largest organelles in the organ (Figure 2(a)). A thin follicular layer ($\bar{x}$ = 156 ± 119 nm, n = 12) surrounded the entire vitellarium and appeared syncytial (Figure 2(d,e)), though several sections revealed the layer to be extremely thin or absent. The layer contained a granular cytoplasm, abundant mitochondria, presumed autophagic bodies, and some profiles of rough endoplasmic reticulum (rER) and Golgi. No nuclei were observed in our sections, though our sections did not include the entire vitellarium due to its size. A thin basal lamina was present outside the follicular layer. The vitellarium had an extremely granular cytoplasm with abundant mitochondria that were mostly distributed around the periphery of the organ. The nuclei had envelopes with numerous pores of ca. 55–69 nm width ($\bar{x}$ = 64.2 ± 4.7 nm, n = 10) (Figure 2(b,c)). Rough endoplasmic reticulum was present as long tubular membranes dispersed throughout the syncytium, but they never formed abundant

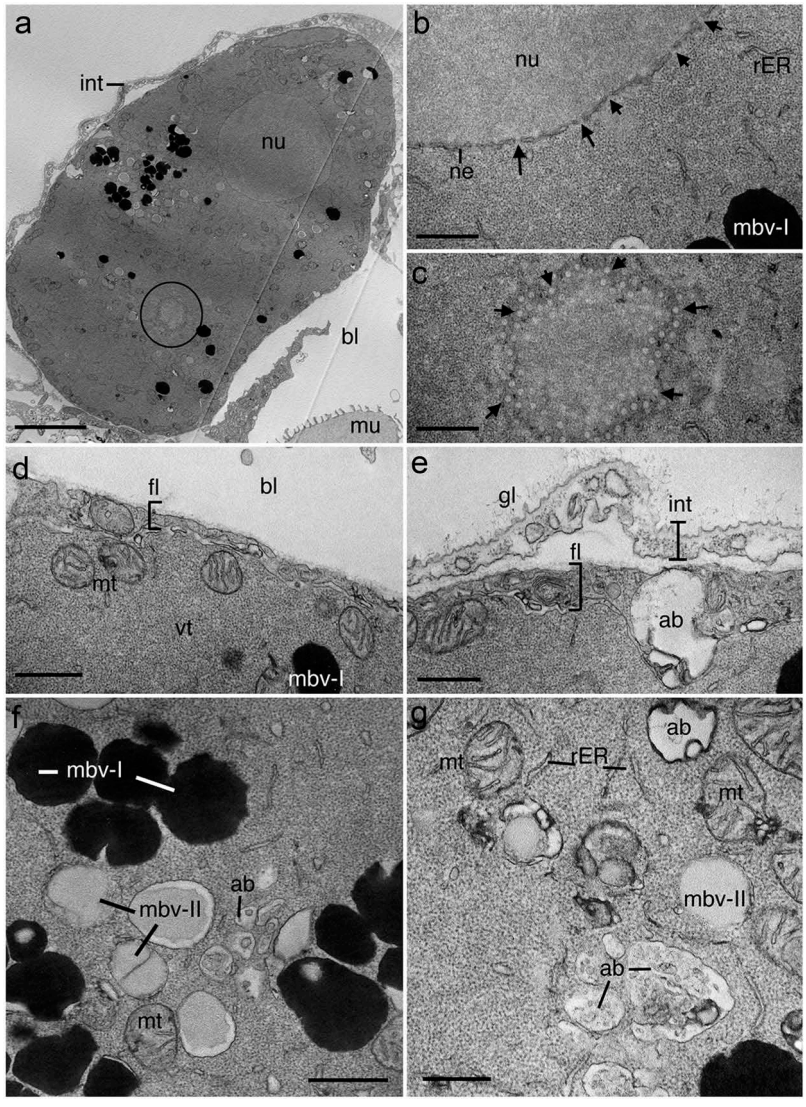

Figure 2. Ultrastructure of the vitellarium of an adult female *Stephanoceros millsii*. (a) Section through the vitellarium showing one large nucleus and a tangential section through the nuclear envelope of a second nucleus (circled, see c). (b) Close up of the nuclear envelope showing nuclear pores (arrows). (c) Tangential section through nuclear envelope revealing nuclear pores (arrows). (d, e) Close ups of follicular layer around the lateral margin of the vitellarium. (f) Two types of membrane-bound vesicles containing either electron dense cores (mbv-I) or light staining flocculent material (mbv-II). (g) Presumed autophagic bodies and other membrane-bound vesicles. Abbreviations: ab: autophagic bodies; bl: blastocoel; gl: glycocalyx; int: integument; fl: follicular layer; mt: mitochondria; mu: muscle; mbv-I: type I membrane-bound vesicle of the vitellarium; mbv-II: type II membrane-bound vesicle of the vitellarium; rER: rough endoplasmic reticulum. Scale bars = A: 3.5 µm; B: 250 nm; C: 350 nm; D: 300 nm; E: 310 nm; F: 615 nm; G: 200 nm.

stacks (Figure 2(b,g)). Golgi was present, but never abundant in the sections we examined. Two types of membrane-bound vesicles were present and appeared to be destined for secretion (Figure 2): type I vesicles (mbv-I) were electron-dense with tight-fitting membranes ($\bar{x}$ = 550 ± 112 nm diameter, n = 14); type II vesicles (mbv-II) contained a light-staining flocculent material bound by a tight-fitting membrane ($\bar{x}$ = 475 ± 90 nm diameter, n = 12); an electron-lucent halo was present around the internal contents of some vesicles. Presumed autophagic bodies were also present in the vitellarium ($\bar{x}$ = 301 ± 147 nm diameter, n = 8), often containing cores with membrane-like structures and undetermined contents. We did not obtain sections through the germarium or maturing oocytes.

Ultrastructure of the embryonic integument and eggshell

A late-stage asexual embryo with corona, mastax, and eyespots visible at the light microscopical level was studied with TEM (e.g., Figure 1(d)). The fixed embryo was slightly contracted within its eggshell although it was unknown whether this was a natural posture or the result of processing for TEM (Figure 3(a,b)). The integument of the embryo was syncytial and bound by an apical plasma membrane that covered an intracellular lamina (ICL), granular cytoplasm, and numerous organelles in the form of membrane-bound vesicles, ribosomes, and mitochondria (Figure 3(c)). Rough endoplasmic reticulum and Golgi were also abundant in the integument and in the subepidermal tissues. The identities of subepidermal tissues were difficult to determine with certainty due to their orientation and state of development, but include the corona (ciliated), infundibulum (ciliated), mastax (with trophi elements), and protonephridia (ciliated) (Figure 3(a,b)).

The thickness of the syncytial integument was highly variable (154–1747 nm, $\bar{x}$ = 451 ± 352 nm, n = 28), with the thinnest regions composed of ICL and a thin strip of underlying cytoplasm, while the thickest regions contained ICL, membrane-bound vesicles, and other signs of secretory activity such as rER and Golgi (Figure 3(c)). Apically, the integument was covered by a thin trilaminar plasma membrane (11.0–15.1 nm, $\bar{x}$ = 13.2 nm, n = 20). The underlying ICL was mostly amorphous or slightly granular in appearance but contained at least one electron-dense band approximately 11–13 nm below the plasma membrane. The ICL was 49–93 nm thick ($\bar{x}$ = 68 nm ± 12 nm, n = 24).

The integument contained several membrane-bound vesicles (mbv, Figure 3) with a similar appearance to those in the vitellarium. Vesicle abundance was quantified over a distance of 111 µm of linear integument across several sections. The number of vesicles was highly variable and ranged from four vesicles/1.6 µm of linear integument to 41 vesicles/22 µm of linear integument (total: 93 vesicles/35. 9 µm of linear integument, $\bar{x}$ = 2.6 vesicles/µm). Most vesicles were relatively oval in shape and varied in size from 83 nm to 258 nm ($\bar{x}$ = 176 nm ± 59 nm, n = 22). Other vesicles were ellipsoid and varied in size: e.g. 83 × 131 nm, 100 × 239 nm, and 177 × 415 nm. Three general categories of vesicles were present based on their contents: 1) Large, electron-dense vesicles (mbv-I) with tight limiting membranes; 2) vesicles with light-staining flocculent (loosely clumped) materials (mbv-II, Figures 3(c) and 4(a,d)); and 3) vesicles with highly variable electron-dense contents (mbv-III, Figures 3(d) and 4(a–d)). 2). The large vesicles (mbv-I) ranged in size from 368 to 582 nm ($\bar{x}$ = 463 nm ± 108 nm, n = 10). They consisted of a homogenous, electron-dense core that did not vary in appearance despite being present in a variety of tissues. Similar vesicles were present in subepidermal tissues and were of similar size to those in the integument (range: 278–661 nm; $\bar{x}$ = 481 ± 192 nm; n = 10). The two other types of vesicles (mbv-II, mbv-III) were more abundant than mbv-I in the integument. Vesicles mbv-II had lightly-staining cores while mbv-III had contents that appeared as electron-dense filaments, dots, or membranes in different configurations (compare Figure 4(b,c)). Many vesicles showed evidence of exocytosis: i.e., where vesicles fused with the apical plasma membrane resulting in a fusion pore through which contents were released into the extra-embryonic space (black arrows, Figures 3(c) and 4(a,c)).

The extra-embryonic space between the integument and the eggshell matrix had a few secretory granules (Figure 4(e)). The granules were similar in electron density to the contents of the membrane-bound vesicles type found in the integument and other tissues (Figures 3(a,b) and 4(d)), but were always smaller and relatively uncommon (range: 59–170 nm, $\bar{x}$ = 122 nm ± 57 nm, n = 5). This space also contained thick, electron-dense fibers that were noticeably different in appearance from the matrix that made up the eggshell (see below).

The eggshell appeared to consist of one layer with two sublayers: an external solid sublayer and an internal flocculent sublayer (Figures 3(c) and 4). The external sublayer was more distinct than the inner sublayer. The apical side of the outer sublayer had a trilaminar appearance with a total thickness from 14 to 26 nm ($\bar{x}$ = 18 nm ± 3 nm, n = 15). The matrix beneath the lamina often appeared granular and in some areas could not be readily distinguished from the inner eggshell sublayer due to their similarities in electron

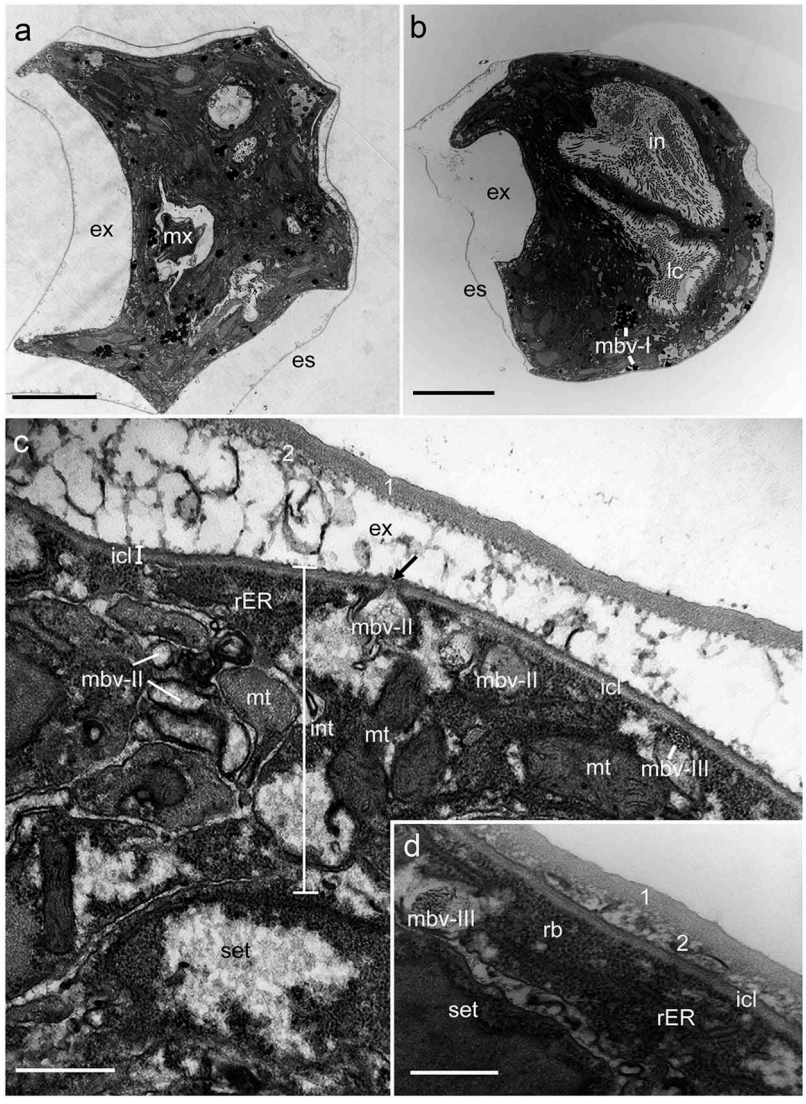

Figure 3. Ultrastructure of a late-stage embryo of *Stephanoceros millsii*. (a) Section of embryo showing mastax region. (b) Section of embryo showing larval corona and infundibulum. (c) Close up of embryonic integument showing the extra-embryonic space between the integument and the eggshell. (d) Close up of embryonic integument where eggshell was in contact with the embryonic integument. Both sublayers are labeled.

Abbreviations: 1: external (outer) eggshell sublayer; 2: internal eggshell sublayer; es: eggshell; ex: extra-embryonic space; icl: intracytoplasmic lamina; in: infundibulum; int: integument; lc: larval corona; mbv-I: membrane-bound vesicles with electron-dense contents; mbv-II, membrane-bound vesicles with light staining flocculent materials; mvb-III: membrane-bound vesicles with variable contents; mt: mitochondria; mx: mastax; rb: ribosomes filling the cytoplasm; rb: ribosomes; rER: rough endoplasmic reticulum; set: subepidermal tissues. Scale bars = A: 10 µm; B: 10 µm; C: 420 nm; D: 300 nm.

density (though the inner matrix was generally more filamentous) (Figure 4(e)). The total shell thickness (including the lamella) of the outer sublayers ranged from 72 to 121 nm ($\bar{x}$ = 93 ± 13 nm, n = 33). The inner sublayer was filamentous and often appeared web-like. This layer adhered to the external layer around much of the eggshell, but in several places appeared to peel away from it (Figures 3(c) and 4(b,e,f)). Consequently, measurements of its thickness (range: 41–178 nm, $\bar{x}$ = 76 ± 32 nm, n = 31) were dependent on how tightly this sublayer adhered to the outer sublayer. Small bundles of filamentous matrix were common below this sublayer (extra-embryonic space), and in several cases, appeared to be the result of exocytosis from membrane-bound vesicles of the integument (Figure 4(a)).

Larval integument

The integument was syncytial and comprised an apical ICL and highly granular cytoplasm. In both the free-swimming larva and newly settled individual (undergoing metamorphosis), the most abundant organelles were ribosomes that imparted a strong granularity to the cytoplasm (Figure 5(a)), while other organelles such

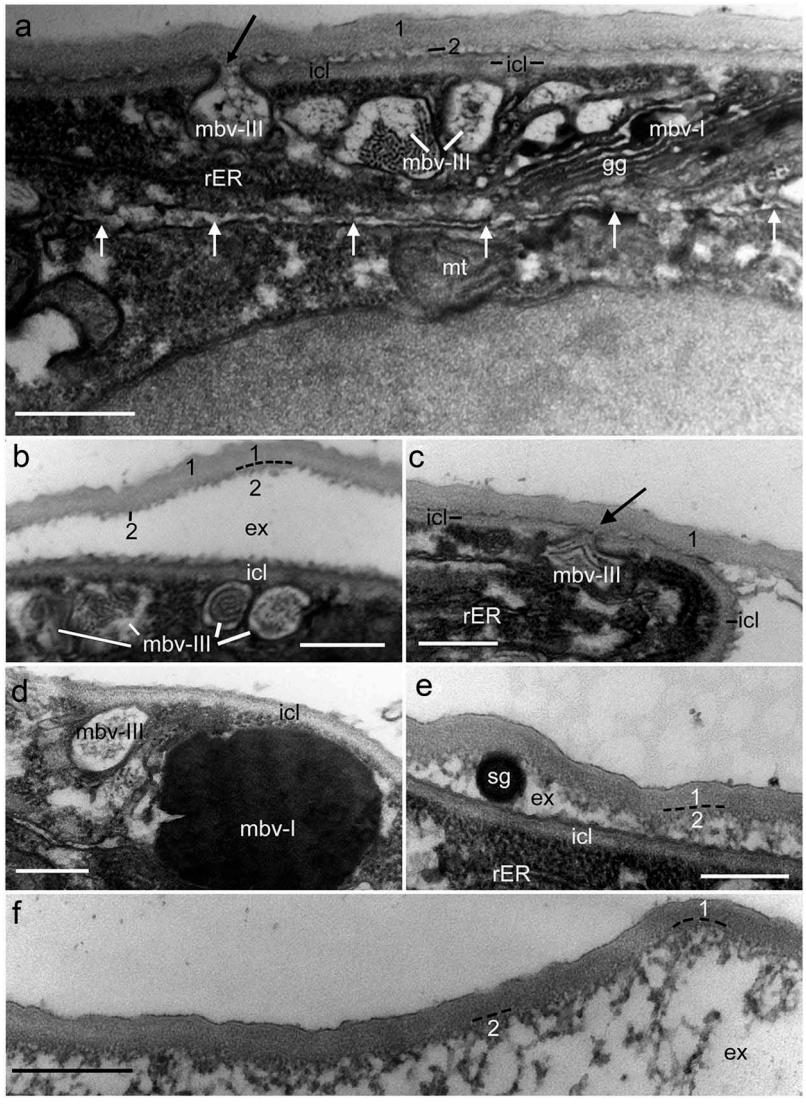

Figure 4. Ultrastructure of the eggshell and integument of the late stage embryo of *Stephanoceros millsii*. (a) Exocytotic activity of membrane-bound vesicles in the integument. Note the presence of flattened stacks of Golgi in proximity to the membrane bound vesicles (mbv-III). White arrows point to the basal plasma membrane of the integument that separates the epidermis from the subepidermal tissues. (b) Membrane-bound vesicles (mbv-III) with a range of electron-dense contents. (c) Two types of membrane-bound vesicles. (d) Membrane-bound vesicles with electron-dense cores and filamentous cores. Eggshell not in view. (e) Electron-dense secretory granule in the extra-embryonic space. (f) Close up of eggshell showing the two sublayers. Integument not in view.

Abbreviations: 1: outer eggshell sublayer; 2: inner eggshell sublayer; rER: endoplasmic reticulum; ex: extra-embryonic space; gg: golgi; icl, intracytoplasmic lamina; mt: mitochondria; mbv-I: membrane-bound vesicle with homogeneous, electron dense contents; mbv-II: membrane-bound vesicle with mostly electron-lucent contents; mbv-III: membrane-bound vesicles with variable electron-dense contents; rER: rough endoplasmic reticulum; sg: secretion granule in extra-embryonic space. Scale bars = A: 360 nm; B: 300 nm; C: 300 nm: 200 nm; E: 250 nm; F: 260 nm.

as mitochondria and membrane-bound vesicles were present but never abundant (Figure 5) except for in the region of the foot (Figure 5(c)). Nuclei and endoplasmic reticulum were also present, but never abundant in any region of the larval integument. The integument had a total thickness of 153–863 nm ($\bar{x}$ = 426 ± 170 nm, n = 10); the thickness of the integument depended on the presence of folds in the body (due to contraction of the larva) and/or the presence of organelles (e.g. membrane-bound vesicles, mitochondria, nuclei). The apical ICL had a thickness of 79–125 nm (=97 ± 19 nm, n = 10) and consisted of an electron-dense outer plasma membrane and slightly less electron-dense granular region. Most of the ICL was relatively flat and without ornaments, though in some regions the ICL showed evidence of a ridge-like pattern (not shown). The ICL was covered with a glycocalyx of 139–226 nm ($\bar{x}$ = 191 ± 33 nm, n = 6) that was present as a thin flocculent and/or filamentous covering (Figure 5(a)). The cytoplasm below the ICL was highly granular across the body, but

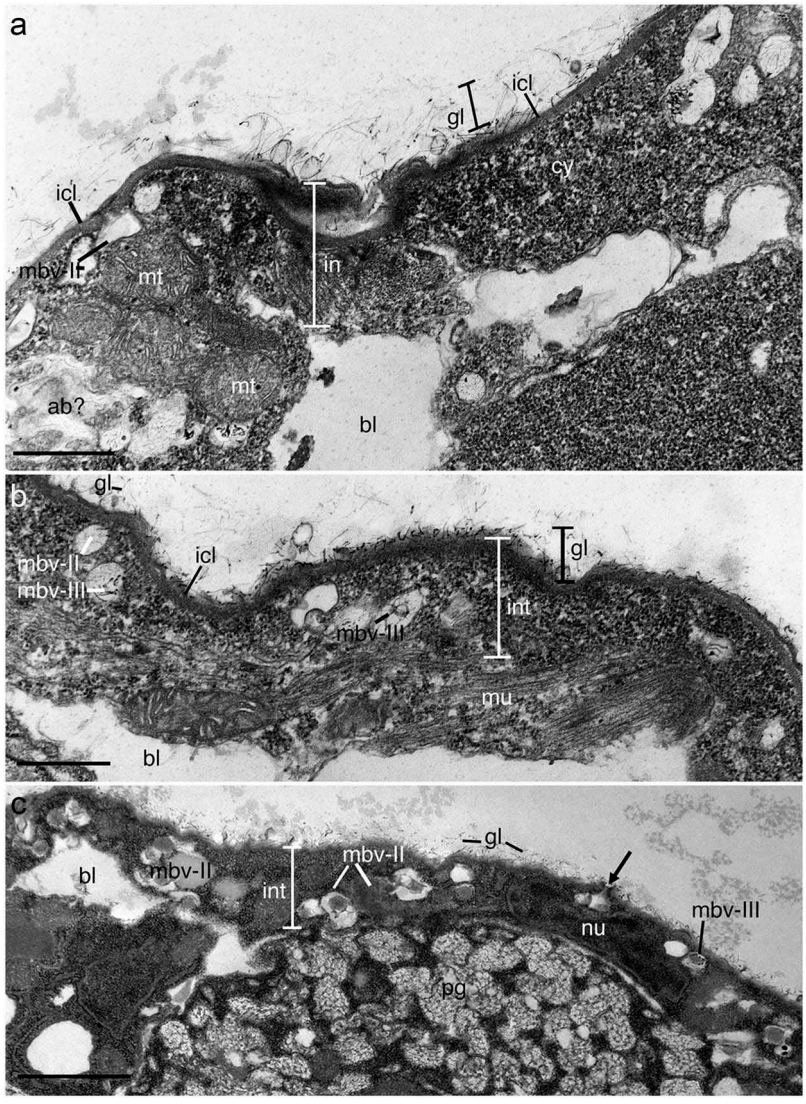

Figure 5. Integument of an asexual female larva of *Stephanoceros millsii*. (a) Integument of the trunk region just posterior of the larval corona. Note the very light and fibrous glycocalyx outside the integument and the granular nature of the cytoplasm. Membrane-bound vesicles of various types are present. (b) Close up of integument from a second larva showing different types of membrane-bound vesicles. Section includes a portion of a longitudinal muscle inserting on the integument. (c) Close up of the foot region in a metamorphosing larva (settled). A black arrow points to a fusion pore created by an underlying membrane-bound vesicle. The integument that is adjacent to the pedal gland shows more membrane-bound vesicles than the integument in the trunk. There is no evidence that secretions from the pedal gland are translocated to the integument for exocytosis.

Abbreviations: ab, autophagic bodies; bl: blastocoel; cy, granular cytoplasm below the icl; gl: glycocalyx; icl: intracytoplasmic lamina; int: integument; mt: mitochondria; nu: nucleus; pg: pedal gland; mbv-I, membrane-bound vesicle with homogeneous, electron dense contents; mbv-II: membrane-bound vesicles with light-staining contents; mbv-III: membrane-bound vesicles with variable electron-dense contents; mu: muscle. Scale bars = A: 700 nm; B: 700 nm; C: 1.1 µm.

noticeably more electron-dense in the foot region by the pedal glands (Figure 5(c)). Membrane-bound vesicles were common and appeared to consist of three main types: potential autophagic bodies (Figure 5(a)), type I membrane-bound vesicles with electron-dense cores (not shown), type II membrane-bound vesicles with light staining cores (Figure 5) and type III membrane-bound vesicles with variable contents (Figure 5(b,c)). The autophagic bodies were often large (>1 µm) and appeared to consist of multiple fused membrane-bound vesicles with different contents (Figure 5(a)). Membrane-bound vesicles, type I were relatively rare, but when present were 68–542 nm ($\bar{x}$ = 308 ± 237 nm). Membrane-bound vesicles type II and III were 126–264 nm in diameter ($\bar{x}$ = 190 ± 48 nm, n = 6) and relatively rare in the trunk region (Figure 5(a,b)), but more abundant in the foot where pedal glands abutted the integument (Figure 5(c)).

Adult integument

The adult epithelium was syncytial. A glycocalyx was present externally and up to 500 nm thick (Figure 6(a,b)). In several sections, the glycocalyx had peeled away from the integument (Figure 6(c,d)). An extracorporeal hydrogel tube was present external of the glycocalyx and consisted of electron-dense lines and dots that gave it a web-like appearance (Figure 6(b)). The integument had a total thickness of 454–1315 nm ($\bar{x}$ = 1031 ± 245 nm, n = 15) in the trunk region; the foot region was not measured. The apical plasma membrane was trilaminar and 17–23 nm thick ($\bar{x}$ = 21 ± 2.4 nm). The ICL was extremely thin and granular in appearance; in many regions it was difficult to distinguish the ICL from the apical plasma membrane and so measurements included both (range: 43–98 nm, $\bar{x}$ = 64 nm ± 11.7 nm). Below the ICL was a highly granular cytoplasm with abundant ribosomes, rER, Golgi, and mitochondria (Figure 6(a,c,d)); nuclei were present, but rare in most sections (Figure 6(c,d)). Membrane-bound vesicles were present in two forms: as type I (mbv-I) vesicles with electron-dense cores and as type II (mbv-II) with electron-lucent cores that often contained lightly stained flocculent materials (Figure 6(c)). Forty-four vesicles were quantified over a linear distance of 36.4 µm (1.21 vesicles/linear µm). Most sections revealed membrane-bound vesicles

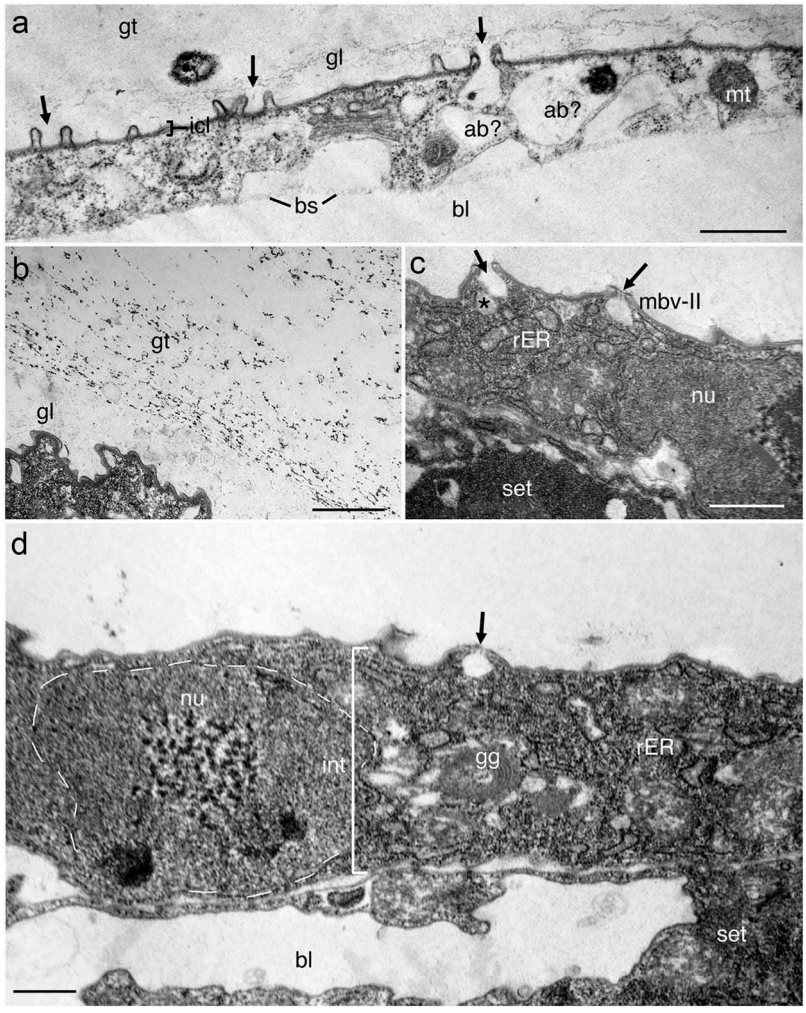

Figure 6. Ultrastructure of the integument of a reproductive adult female *Stephanoceros millsii*. (a) Integument showing high levels of secretion activity by the presence of multiple exocytotic vesicles forming finger-like projections (black arrows) of the apical plasma membrane and ICL. (b) Close up of the glycocalyx (extremely light staining) and extracorporeal tube (electron-dense lines and dots) external to it. (c) Close up view of a region of the integument with a nucleus, abundant rough endoplasmic reticulum, and secretion vesicles. (d) Active integument with nucleus (artificially outlined), golgi, and rough endoplasmic reticulum.

Abbreviations: *: region of fusion of membrane-bound vesicle containing flocculent material (mbv-II) with a vesicle that produced a fusion pore; ab: autophagic body; bl: blastocoel; bs: basal lamina; black arrow: exocytosis pore formed from membrane-bound vesicle; gg: golgi; gl: glycocalyx; icl: intracytoplasmic lamina (extremely thin); mbv-II: membrane-bound vesicle with electron-lucent contents; mt: mitochondria; nu: nucleus; rER: rough endoplasmic reticulum; set: subepidermal tissue. Scale bars = A: 400 nm; B: 500 nm; C: 600 nm; D: 500 nm.

fusing with the overlying ICL to create a fusion pore (black arrows, Figure 6(c)); this fusion created small ($\bar{x}$ = 131 ± 11 nm) finger-like projections of the apical plasma membrane/ICL (Figure 6(a)) where exocytosis occurred. Type I membrane-bound vesicles were relatively rare, but when present were between 349 to 584 nm in diameter. The basal portion the integument was highly irregular in outline and in some regions appeared to be in the process of either endocytosis or exocytosis (Figure 6(a)); membrane-bound vesicular pockets were present above the thin basal lamina. Some of these vesicles might be autophagic bodies because they appeared to contain degraded materials (Figure 6(a)); the identities of these materials could not be ascertained.

Discussion

Monogonont rotifers produce two general types of eggs during their life cycle: subitaneous (amictic) eggs that hatch quickly as clonal females and mictic eggs that hatch as haploid males if unfertilized, or if fertilized, hatch as females after a period of developmental arrest (i.e. diapausing or resting eggs). Resting eggs are capable of enduring harsh environmental conditions (reviewed by Gilbert 1983). Most research on rotifer eggs has focused on factors that regulate egg production (e.g. reviewed by Snell 2011; Stelzer 2017), while detailed studies of oogenesis are comparatively rare and focus on few taxa (Tannreuther 1920; Nachtwey 1925; Hsu 1956a, 1956b; Lechner 1966; Bentfield 1971a, 1971b; Amsellem and Ricci 1982; Pagani et al. 1993; Boschetti et al. 2005; Smith et al. 2010). Ultrastructural studies of eggshells are even more infrequent (Wurdak et al. 1977, 1978; Gilbert 1995; reviewed in Clément and Wurdak 1991). The fact that so little information is available on the ultrastructure of rotifer eggshells is surprising given their importance in regulating the internal environment, protecting the embryo from predation, desiccation, and freezing, and even permitting the entry of select environmental cues (Kim et al. 2015).

Most rotifer eggshell precursors are produced in the syncytial vitellarium during oogenesis, and along with other organelles are directed with the vitellous flow to individual oocytes through cytoplasmic bridges (Bentfield 1971b, Ammselem and Ricci 1982; Clément and Wurdak 1991). Membrane-bound vesicles discharge these precursors via exocytosis to the surface of the oocyte after its separation from the germarium/ovarium (Clément and Wurdak 1991). Details on eggshell precursors are scant; their chemical identities are largely unknown although early studies have shown the presence of chitin in select eggshell membranes that are produced by the embryo (Depoortere and Magis 1967; Piavaux 1970; Piavaux and Magis 1970). There is no information on how the precursors form the shell and there is no indication when shell formation stops: i.e. in the zygote stage or at some point during embryogenesis (Gilbert 1983).

To date, the only studies of eggshell ultrastructure (beyond the fine structure of the eggshell surface) come from investigations of motile species including *Asplanchna sieboldii* (Leydig, 1854) (Wurdak et al. 1977, 1978), *Brachionus calyciflorus* Pallas, 1766 (Wurdak et al. 1977, 1978), *Brachionus plicatilis* Müller, 1786 and *Brachionus rotundiformis* Tschungunoff, 1921 (Munuswamy et al. 1996), *Notommata copeus* Ehreneberg, 1834 (Clément and Wurdak 1991), *Synchaeta pectinata* (Gilbert 1995), and *Trichocerca rattus* Müller, 1786 (Clément and Wurdak 1991). Among these species, only the studies of *S. pectinata* and *T. rattus* provide data on the ultrastructure of subitaneous eggs, while all other studies are either focused on resting eggs or do not provide any description of the subitaneous eggshells (Wurdak et al. 1977). The eggshells of *S. pectinata* and *T. rattus* appear to consist of two layers, but these layers are structurally different. The subitaneous eggshells of *S. pectinata* have an external mucilaginous coat (~30 µm thick), but the shell itself consists of an inner striated sublayer and an outer sublayer of rod-like elements with fine filaments; total shell thickness reaches 1.4 µm (Gilbert 1995). The eggshell of *T. rattus* lacks a mucilaginous coat and consists of two layers separated by a gap: it has a thick external later that forms the hardened shell and a thin membranous envelope that lines the embryo (measurements were not provided, Clément and Wurdak 1991). In our study of a sessile rotifer's subitaneous eggshell, we demonstrated the presence of a single layer with two tightly adjoining sublayers: an outer (solid) sublayer of 72–121 nm thickness and an inner flocculent sublayer of 41–178 nm thickness (Figure 2(c)). No membrane-like envelope was observed. The outer sublayer had an apical trilaminar appearance that accounted for approximately 10–30% of its thickness; this sublayer was devoid of any external ornamentation. The flocculent sublayer was highly variable in thickness; in most sections, this layer was adjacent to the outer sublayer, but in other sections, the flocculent sublayer had peeled away and revealed a filamentous and slightly web-like appearance that spanned the extra-embryonic space. We are uncertain whether the extra-embryonic space is natural or an artifact of fixation. No microvilli were observed on the embryonic integument.

To get a better sense about the diversity of eggshell ultrastructure among rotifers, we compare these results to ultrastructural data on resting eggs, even though such eggs are well known to be more complex.

Observations of *A. sieboldii* reveal the resting eggshell to be composed of two main layers (each with sublayers): an outer layer that forms the external ornamentation and is more than 20 µm thick, and an inner layer that is mostly granular, but connected to the outer layer through stalks. A fine meshwork of fibers is present between the internal layer and the egg cytoplasm (Wurdak et al. 1977). Species of *Brachionus* appear to have 2–3 layers (with sublayers) depending on interpretation: an outer electron-dense layer (2–5 µm) that forms a lattice-like network; a middle layer (400–500 nm) that is mostly homogeneous; and an undulating inner layer (40 nm) that borders the embryo (and may be a membrane). A space separates the middle layer from the inner layer and contains granular material and fibrils that are bound to the middle layer. *Synchaeta pectinata* is capable of producing an asexual, diapausing embryo with an eggshell composed of a single complex layer up to 9 µm thick and includes an outer zone (sublayer 1) that forms perpendicular rods with fine filaments, and an inner striated zone (sublayer 2) (Gilbert 1995).

It is apparent from these descriptions that eggshell ultrastructure, whether subitaneous or diapausing, is extremely diverse among rotifers. Our results on the subitaneous egg of *S. millsii* reveal an eggshell that is generally under 200 nm in thickness, depending on how tightly the inner sublayer adjoins the outer sublayer. The external sublayer is not obviously striated and its core matrix is mostly granular, making its ultrastructure dissimilar in many respects to the eggshell layers described for other species. We note that the outer sublayer has a similar appearance (staining quality) to the type II membrane-bound vesicles in the maternal vitellarium and embryo, but we are uncertain whether these vesicles are secretory, and if so, are destined for eggshell production. The maternal vitellarium and embryo also had membrane-bound vesicles (type-I) with electron-dense cores that are similar to the cortical granules described for other species (see Gilbert 1983), but we are uncertain of their function or destination; i.e., for exocytosis to the eggshell. Despite these uncertainties, we are confident that the late stage embryo continues to engage in secretion even after the outer eggshell sublayer is apparently fully formed. Several sections revealed fusion pores between vesicles and the integument (black arrows, Figure 3–5), which would seem to indicate exocytosis of the contents, most of which are in the form of flocculent material (mbv-II, Figure 4(a)), but are sometimes present as membrane-like lamellae (mbv-III, Figure 4(b,c)) or electron-dense granules (mbv-III, Figure 4(d)). These latter contents were characteristic of vesicles we call type III, which are present in both the embryo and larva. The flocculent material appears to be destined for the inner eggshell sublayer based on similar staining qualities and morphology, but we are unsure of the destination of the dot-like and lamellar contents.

Why such a late stage embryo – a near fully formed larva – continues to secrete so late into development is a mystery. According to Wurkdak et al. (1978), newly hatched rotifers are often encased in a hatching membrane that is secreted during embryogenesis, and this membrane may function to protect the neonate from harm as it breaks through the eggshell. Whether this hatching membrane is the same as the (flocculent) inner eggshell envelope is unknown. If all rotifers do have hatching membranes, then some of the secretions (perhaps flocculent inner layer) of *S. millsii* may in fact be contributing to the hatching membrane. However, we have not seen a hatching membrane in this species at the light microscopical level, unless this membrane is destined to become part of the larval glycocalyx, which is similarly flocculent. We do note that the larval integument is less active than (1.08 membrane-bound vesicles/linear µm) than the embryonic integument (2.59 membrane-bound vesicles/linear µm), which may be indicative of the precocious production of the larval glycocalyx (and hatching membrane?) in preparation for exiting the eggshell and eventual environmental exposure. Whether the lamellar contents of type III vesicles are also destined for exocytosis to contribute to the glycocalyx, or perhaps the ICL, remains unknown.

Our observations further reveal that the rotifer's glycocalyx continues to thicken after metamorphosis and into adulthood, but the adult integument and ICL do not appear to thicken substantially. Still, the integument is extremely active as noted by the presence of abundant ribosomes, rough endoplasmic reticulum, and Golgi; membrane-bound vesicles are present throughout the animal's epidermis and we observed exocytosis in the form of vesicle fusion with the plasma membrane (Figure 6). Our estimates of the abundance of membrane-bound secretion vesicles (1.21 secretion vesicles/linear µm) in the adult are lower than the embryo, but slightly higher than the larva. Regardless, some of the flocculent secretions released via exocytosis are similar in structure and staining quality to the glycocalyx. Importantly, we have found that the adult glycocalyx is not the same secretion as the thick extracorporeal tube that surrounds the adult rotifer's body (Figure 1(a)). Instead, our preliminary data indicate that the extracorporeal tube has a different site of secretion, likely to be in the foot region and consist of pedal gland secretions and specializations of the integument (Yang pers. obs.).

Based on these results, we hypothesize that secretory activity in the rotifer integument as measured by the relative amount of vesicle trafficking observed with TEM varies during a sessile species' ontogeny. This vesicle trafficking probably reflects the requirements of the different life stages: eggshell secretion and (possibly) glycocalyx/hatching membrane production in the embryo; glycocalyx maintenance and ICL production (?) during the brief larval period; and finally, the ramping up of glycocalyx production in pre-reproductive and reproductive adults. The adult glycocalyx may serve as a second layer of defense beneath the extracorporeal tube. We note that oviposition by the adult rotifer often results in the eggs being positioned between the adult glycocalyx and the extracorporeal tube. The thickness of the glycocalyx might therefore prevent the eggshells from damaging the adult's body, particularly the foot.

In conclusion, we recommend that the ultrastructure of rotifer eggshells be considered a worthy topic of investigation that will provide insights into the adaptive value of different egg morphologies and their underlying sexual strategies (Gilbert 1995). The fine external structure of rotifer eggs is already a source of taxonomic information, but determining homology of external shell features that are visible with light microscopy and SEM will likely require studies of eggshell secretion in closely related species (Munuswamy et al. 1996) and more distant taxa (Wurdak et al. 1977, 1978; Gilbert 1995). Additionally, a study of eggshell ultrastructure might provide insights into the evolution of extracorporeal tubes, which are highly diverse among sessile rotifers. These tubes are hypothesized to function for camouflage and/or defense of the adult (Wallace et al. 2015; Yang and Hochberg 2018), but another function may be protection of developing embryos. Further studies on the eggshells of subitaneous embryos in these species are necessary to confirm their simplistic ultrastructure and determine whether such simplicity is characteristic of species with protective tubes.

Acknowledgments

The authors thank the editor and two anonymous reviewers for their constructive criticisms of this manuscript.

Disclosure statement

No potential conflict of interest was reported by the authors.

Funding

This research was supported by the National Science Foundation (NSF) to Rick Hochberg [DEB 1257110], Elizabeth J Walsh [DEB 1257068] and Robert L Wallace [DEB 1257116] and the National Institutes on Minority Health and Health Disparities [5G12MD007592], a component of the National Institutes of Health (NIH). Any opinions, findings, and conclusions or recommendations expressed in this material are those of the authors and do not necessarily reflect the views of the NSF and NIH;Division of Environmental Biology [1257068,1257110,1257116];National Institute on Minority Health and Health Disparities [5G12MD007592].

ORCID

Rick Hochberg http://orcid.org/0000-0002-5567-5393
Hui Yang http://orcid.org/0000-0002-0491-5123
Elizabeth J. Walsh http://orcid.org/0000-0002-6719-6883
Robert L. Wallace http://orcid.org/0000-0001-6305-4776

References

Amsellem J, Ricci C. 1982. Fine structure of the female genital apparatus of *Philodina* (Rotifera, Bdelloidea). Zoomorphology. 100:89–105.

Bentfield ME. 1971a. Studies of oogenesis in the rotifer *Asplanchna* I. Fine structure of the female reproductive system. Z Zellforch Microsk Anat. 115:165–183.

Bentfield ME. 1971b. Studies of oogenesis in the rotifer *Asplanchna* II. Oocyte growth and development. Z Zellforch Microsk Anat. 115:184–195.

Birky CW Jr., Gilbert JJ. 1971. Parthenogenesis in rotifers: the control of sexual and asexual reproduction. Integr Comp Bio. 11:245–266.

Boschetti C, Leasi F, Ricci C. 2011. Developmental stages in diapausing eggs: an investigation across monogonont rotifer species. Hydrobiologia. 662:149–155.

Boschetti C, Ricci C, Stoga C, Fascio U. 2005. The development of a bdelloid egg: a contribution after 100 years. Hydrobiologia. 546:323–331.

Brodie AE. 1970. Development of the cuticle in the rotifer *Asplanchna brightwelli*. Z Zellforch Microsk Anat. 105 (4):515–525.

Clément P. 1980. Phylogenetic relationships of rotifers, as derived from photoreceptor morphology and other ultrastructural analyses. Hydrobiologia. 73:93–117.

Clément P, Wurdak E. 1991. Rotifera. In: Harrison FW, Ruppert EE, editors. Microscopic anatomy of invertebrates. Volume 4. Aschelminthes. New York: Wiley-Liss; p. 219–297.

Depoortere H, Magis N. 1967. Mise en evidence, localization et dosage de la chitine dans la coque des oeufs de *Brachionus leydigii* Cohn et d'autres rotiferes. Ann Soc R Zool Belg. 97:187–195.

Gilbert JJ. 1974. Dormancy in rotifers. Trans Am Microsc Soc. 93:490–513.

Gilbert JJ. 1983. Rotifera. In: Adiyodi KG, Adiyodi RG, editors. Reproductive biology of invertebrates. Volume 1: oogenesis, oviposition, and oosorption. New York: John Wiley and Sons; p. 181–209.

Gilbert JJ. 1989. Rotifera. In: Adiyodi KG, Adiyodi RG, editors. Reproductive biology of invertebrates. Volume IV, Part A: fertilization, development, and parental care. New Delhi: Oxford & IBH Publishing Cop. Pvt. Ltd; p. 179–199.

Gilbert JJ. 1995. Structure, development and induction of a new diapause stage in rotifers. Freshwater Biol. 34:263–270.
Gilbert JJ. 2002. Endogenous regulation of environmentally induced sexuality in a rotifer: a multigenerational parental effect induced by fertilization. Freshwater Biol. 47:1633–1641.
Gilbert JJ. 2003. Environmental and endogenous control of sexuality in a rotifer life cycle: developmental and population biology. Evol Dev. 5:19–24.
Gilbert JJ. 2004. Population density, sexual reproduction and diapause in monogonont rotifers: new data for *Brachionus* and a review. J Limnol. 63:32–36.
Gómez A, Carvalho GR. 2001. Sex, parthenogenesis and genetic structure of rotifers: microsatellite analysis of contemporary and resting egg bank populations. Mol Ecol. 9:203–214.
Hairston NG Jr. 1996. Zooplankton egg banks as biotic reservoirs in changing environments. Limnol Oceanogr. 41:1087–1092.
Hochberg A, Hochberg R. 2015. Serotonin immunoreactivity in the nervous system of the free-swimming larvae and sessile adult females of stephanoceros fimbriatus (rotifera: gnesiotrocha) . Invertebr Biol. 134:261–270. doi:10.1111/ivb.12102
Hsu WS. 1956a. Oogenesis in the Bdelloidea rotifer *Philodina roseola* Ehrenberg. Cellule. 57:283–296.
Hsu WS. 1956b. Oogenesis in *Habrotrocha tridens* (Milne). Biol Bull. 111:364–374.
Jennings HJ. 1896. The early development of *Asplanchna herrickii* de Guerne. A contribution to developmental mechanics. Bull Mus Comp Zool. 30:1–117.
Kim H-J, Suga K, Kim B-M, Rhee J-S, Lee J-S, Hagiwara A. 2015. Light-dependent transcriptional events during resting egg hatching of the rotifer *Brachionus manjavacas*. Mar Genomics. 20:25–31.
Koehler JK. 1965. A fine structure study of the rotifer integument. J Ultrastruct Res. 12:113–134. doi:10.1016/S0022-5320(65)80011-9
Kutikova LA. 1995. Larval metamorphosis in sessile rotifers. Hydrobiologia. 313/314 :133–138. doi:10.1007/BF00025942
Lechner M. 1966. Untersuchungen zur Embryonalenentwicklung des Rädertieres *Asplanchna girodi* de Guerne. Wilhelm Roux Arch Entwickl Mech Org. 157:117–173.
Lopes PM, Bozelli R, Bini LM, Santagelo JM, Decleck S. 2016. Contributions of airborne dispersal and dormant propagule recruitment to the assembly of rotifer and crustacean zooplankton communities in temporary ponds. Freshwater Biol. 61:658–669.
Mark Welch DB, Ricci C, Meselson M. 2009. Bdelloid rotifers: progress in understanding the success of an evolutionary scandal. In: Schön I, Martens K, Dijk P, editors. Lost Sex. Dordrect: Springer; p. 259–279.
Munuswamy N, Hagiwara A, Murugan G, Hirayama K, Dumont HJ. 1996. Structural differences between the resting eggs of *Brachionus plicatilis* and *Brachionus rotundiformis* (Rotifera, Brachionidae): an electron microscopic study. Hydrobiologia. 318:219–223.
Nachtwey R. 1925. Untesuchungen über die Keimbahn, Organogenese und Anatomie von *Asplanchna priodonta* Gosse. Z Zellforch Microsk Anat. 126:239–492.
Pagani M, Ricci C, Redi CA. 1993. Oogenesis in *Macrotrachela quadricornifera* (Rotifera, Bdelloidea). I. Germarium eutely, karyotype, and DNA content. Hydrobiologia. 255/256:225–230.
Piavaux A. 1970. Origine de l'enveloppe chitineuse des oeufs de deux rotiféres du genre *Euchlanis* Ehrenberg. Ann Soc R Zool Belg. 100:129–137.
Piavaux A, Magis N. 1970. Données complémentaires sur la localisation de la chitine dans les enveloppes des oeufs de rotiféres. Ann Soc R Zool Belg. 100:49–59.
Ricci C. 2001. Dormancy patterns of rotifers. Hydrobiologia. 446:1–11.
Rivas JA Jr., Mohl J, Leung MY, Wallace RL, Gill TE, Walsh EJ. 2018. Evidence for regional aeolian transport of freshwater biota in arid regions. Limnol Oceanogr Lett. 3(4):323–330.
Schramm U. 1978. Studies on the ultrastructure of the integument of the rotifer habrotrocha rosa donner (aschelminthes). Cell Tiss Res. 189:167–177.
Smith JM, Cridge AG, Dearden PK. 2010. Germ cell specification and ovary structure in the rotifer *Brachionus plicatilis*. EvoDevo. 1:5.
Snell T. 1987. Sex, population dynamics and resting egg production in rotifers. Hydrobiologia. 144:105–111.
Snell T. 2011. A review of the molecular mechanisms of monogonont rotifer reproduction. Hydrobiologia. 662:89–97.
Stelzer CP. 2017. Life history variation in monogonont rotifers. In: Hagiwara A, Yoshinaga T, editors. Rotifers. Fisheries science series. Singapore: Springer; p. 89–109.
Storch V, Welsch U. 1960. Über den Aufbau des Rotatorienintegumentes. Z Zellforsch Mikrosk Anat. 95:405–414.
Tannreuther GW. 1920. The development of *Asplanchna ebbersbornii* (rotifer). J Morph. 33:389–422.
Wallace RL, Snell T, Ricci C, Nogrady T. 2006. Rotifera. Volume 1: biology, ecology and systematics. In: Segers H, editor. Guides to the identification of the microinvertebrates of the continental waters of the world, No. 23. 2nd ed. Leiden: Backhuys Publishers; p. 299.
Wallace RL, Snell T, Smith HA. 2015. Phylum Rotifera. In: Thorp JH, Rogers DC, editors. Thorp and covich's freshwater invertebrates, Vol. I., ecology and general biology. Waltham (MA): Elsevier; p. 225–271.
Walsh EJ. 1989. Oviposition behavior of the littoral rotifer *Euchlanis dilatata*. Hydrobiologia. 186:157–161.
Walsh EJ, May L, Wallace RL. 2017. A metadata approach to documenting sex in phylum Rotifera: diapausing embryos, males, and hatchlings from sediments. Hydrobiologia. 796:265–276.
Walsh EJ, Smith HA, Wallace RL. 2014. Rotifers of temporary waters. Int Rev Hydrobiol. 99:3–19.
Wurdak E. 2017. External morphology of the eggs of *Asplanchnopus multiceps* (Schrank, 1793) (Rotifera): solving the 150-year old case of mistaken identity. Hydrobiologia. 796:161–168.
Wurdak E, Gilbert JJ, Jagels R. 1977. Resting egg ultrastructure and formation of the shell in *Asplanchna sieboldi* and *Brachionus calyciflorus*. Arch Hydrobiol Beih. 8:298–302.
Wurdak ES, Gilbert JJ, Jagels R. 1978. Fine structure of the resting eggs of the rotifers *Brachionus calyciflorus* and *Asplanchna sieboldi*. Trans Am Microsc Soc. 97:49–72.
Yang H, Hochberg R. 2018. Ultrastructure of the extracorporeal tube and "cement glands" in the sessile rotifer limnias melicerta (rotifera: gnesiotrocha). Zoomorphology. 137:1–12. doi:10.1007/s00435-017-0371-x
Young A, Hochberg R, Walsh EJ, Wallace RL. 2019. Modeling the life history of sessile rotifers: larval substratum selection through reproduction. Hydrobiologia. doi:10.1007/s10750-018-3802-x